Hindawi Publishing Corporation
Journal of Thermodynamics
Volume 2014, Article ID 670186, 16 pages
http://dx.doi.org/10.1155/2014/670186

Research Article

Separation of Methylene Blue Dye from Aqueous Solution Using Triton X-114 Surfactant

Arunagiri Appusamy,[1] Prabisha Purushothaman,[1] Kalaichelvi Ponnusamy,[1] and Anantharaj Ramalingam[2]

[1]*Department of Chemical Engineering, National Institute of Technology, Tiruchirappalli, Tamilnadu 620015, India*
[2]*Department of Chemical Engineering, Faculty of Engineering, University of Malaya, Kuala Lumpur 50603, Malaysia*

Correspondence should be addressed to Anantharaj Ramalingam; anantharaj@um.edu.my

Received 21 August 2014; Revised 9 November 2014; Accepted 11 November 2014; Published 2 December 2014

Academic Editor: Felix Sharipov

In this study, the interaction energy between Triton X-114 surfactant + methylene blue or water and methylene blue + water was investigated using Hartree-Fock (HF) theory with 6-31G* basis set. The results of structures and interaction energies show that these complexes have good physical and chemical interactions at atom and molecular levels. However, the Triton X-114 surfactant + methylene blue complex shows stronger molecular interaction compared to other complexes systems. The order of the interaction energy is 4303.472023 (Triton X-114 surfactant + water) > −1222.962 (methylene blue + water) > −3573.28 (Triton X-114 surfactant + methylene blue) kJ·mole^{-1}. Subsequently, the cloud point extraction was carried out for 15 ppm of methylene blue in a mixture at 313.15 and 323.15 K over the surfactant concentration range from 0.01 M to 0.1 M. From the measured data, the excess molar volume was calculated for both phases. The results show a positive deviation in the dilute phase and a negative deviation in the surfactant rich phase. It is confirmed that the interaction between Triton X-114 and methylene blue is stronger than other complex systems due to the presence of chemical and structural orientation. The concentration of dyes and surfactant in the feed mixture and temperature effect in both phases has been studied. In addition, the thermodynamics feasibility and efficiency of the process have also been investigated.

1. Introduction

The removal of dyes such as methylene blue (MB) from industrial wastewater before discharge is of uttermost importance. Organic dyes colorize other substances in water, making them visible and aesthetically unpleasant [1]. Besides, photosynthetic activities are hampered due to interference with sunlight penetration into water bodies, thus affecting fish and other aquatic organisms. Ghosh and Bhattacharyya [2] reported that MB is not strongly hazardous but it has very harmful effects on living things. Therefore, the removal of MB from waste water is an essential task. Some of the dyes are carcinogenic and mutagenic due to their molecular structure, functional group, and types such as benzidine and metals [3]. There are serious adverse effects with far-reaching consequences that are attributed to MB. The contact with eye can lead to permanent blindness to human and animals, experiencing short period of rapid or difficult breathing when inhaled, burning sensation when ingested through mouth, and causes other adverse conditions such as nausea, vomiting, profuse sweating, and mental confusion.

Due to recent increase in industrial activities such as textile manufacturing, the use of dyes increases rapidly. The most recent statistics [4] indicated rapid use of these dyes with more than 10,000 different types of dyes being produced. They reported a global annual manufacture of these dyestuffs and intermediates estimated to be 7×10^8 kg. Therefore, the removal of dyes from wastewater is gaining research interest. Removal of these dyes from wastewater effluents is problematic as they possess a complex aromatic chemical structure that makes them highly visible and reduced photosynthetic activity in aquatic systems by reducing light

Table 1: Equation used in this study.

Name	Formula	
Binding energy (BE)	$\mathrm{BE}_{S-D} = \mathrm{TE}_{S+D} - (\mathrm{TE}_S + \mathrm{TE}_D)$	(a)
Excess molar volume (V_E)	$V_E = \sum_{i=1}^{3} \frac{x_i M_i}{\rho_{\mathrm{mix}}} - \sum_{i=1}^{3} \frac{x_i M_i}{\rho_i}$	(b)
Phase volume ratio (R_v)	$R_v = \frac{V_s}{V_w}$	(c)
Pre concentration factor (f_c)	$f_c = \frac{V_t}{V_s}$	(d)
Distribution coefficient (K_d)	$K_d = \frac{C_s}{C_w}$	(e)
Cloud point extraction efficiency (η)	$\eta = \frac{C_0 V_t - C_w (V_t - V_s)}{C_0 V_t} \times 100$	(f)
Change in Gibbs free energy (ΔG^0), change in entropy (ΔS^0), and Change in enthalpy (ΔH^0)	$\Delta G^0 = \Delta H^0 - T\Delta S^0$	(g)
	$\log\left(\frac{q_e}{C_e}\right) = \frac{\Delta S^0}{2.303R} - \frac{\Delta H^0}{2.303RT}$	(h)
	Where: $q_e = \frac{A}{X}$, $A = V_0 C_0 - V_d C_e$, $X = C_s V_0$	

Note: *S*: surfactant; *D*: dyes.

penetration. Several methods have been employed. Some of these techniques are chemical coagulation or flocculation, ozonation, adsorption, oxidation processes, nanofiltration, chemical precipitation, ion-exchange, reverse osmosis, and ultrafiltration. All of these methods either are operationally expensive, inefficient in the removal of the dyes, or create disposal problems. In the last decade, increasing interest in the use of aqueous micellar solution has been found in the field of separation science [5]. Cloud point extraction (CPE) can be used for removing dye from aqueous solution. Such a method offers some advantages over conventional liquid-liquid extraction (LLE), including high extraction efficiency, ease of waste disposal, and the use of nontoxic and less dangerous reagents such as surfactant.

Above the cloud point temperature, aqueous solution of a nonionic surfactant separates into two phases, namely, a surfactant rich phase, which has small volume compared to the solution and is called coacervate phase, and the other is dilute bulk aqueous phase containing surfactant concentration slightly above the critical micelle concentration (CMC) [6]. The dye molecules present in aqueous solution of nonionic surfactant are distributed between the two phases above the cloud point temperature [7]. This phenomenon is known as the cloud point extraction (CPE). The dyes are solubilized in the coacervate phase, and the dye free aqueous dilute phase can be disposed of.

The physical properties of binary mixtures have been studied for many reasons. The most important reason is to provide information about the molecular interactions between similar and dissimilar structure of the molecules in the mixture [8]. In addition, the density, viscosity, and refractive index are essential to understand the thermodynamic behavior of solute or solvent in liquid mixtures [9–13]. The study of excess thermodynamic properties is of considerable interest in understanding the intermolecular interactions in liquid mixtures [14]. For example, excess molar volumes, which depend on the composition and/or temperature, are of great importance in understanding the nature of molecular aggregation that exists in the mixtures. V_E is the resultant contributions from several opposing effects [15]. These may be divided arbitrarily into three types, namely, chemical, physical, and structural ones. Physical contributions, which are nonspecific interactions between the real species present in the mixture, contribute a positive term to V_E. The chemical or specific intermolecular interactions result in a volume decrease, and these include charge-transfer type forces and other complex forming interactions. This effect contributes negative values to V_E. The structural contributions are mostly negative and arise from several effects, especially from interstitial accommodation and changes of free volume. In other words, structural contributions arising from the geometrical fitting of one component into the other due to the differences in the free volume and molar volume between components lead to negative contribution to V_E. The increase in excess molar volume with increasing dipole-dipole interactions is stronger in higher hydrogen bonding.

In this work, the binding energy (Table 1) in mixtures of Triton X-114 surfactant + MB, Triton X-114 surfactant + water, and MB + water complex systems were investigated using Hartree-Fock (HF) Theory with 6-31G* basis set. Subsequently, the density, viscosity, and refractive index were measured at different concentrations of surfactant and four different temperatures. Furthermore, the effects of various design parameters such as dye concentration, surfactant concentration, electrolyte concentration, and cloud point temperature on the phase volume ratio, preconcentration

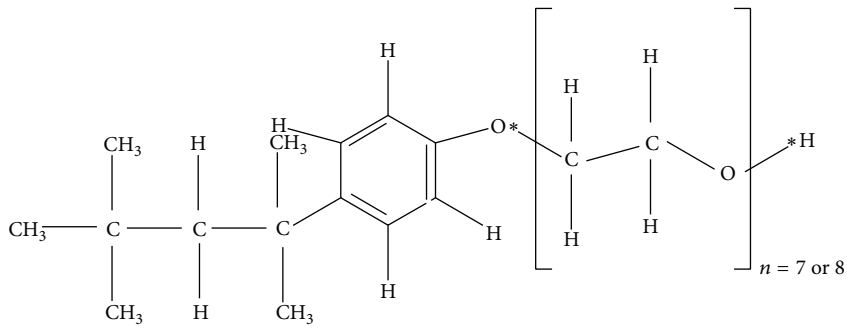

Figure 1: Chemical structure of Triton X-114.

factor, distribution coefficient, and extraction efficiency were calculated (Table 1). Lastly, various thermodynamic parameters such as the change in enthalpy, entropy, and Gibbs free energy were also determined (Table 1).

2. Computational Details

MOLDEN visualization packages [16] have been used to prepare the chemical structure of Triton X-114 surfactant, MB, and water. The complex systems of Triton X-114 surfactant + MB, Triton X-114 surfactant + water, and MB + water were initially drawn by using dummy atoms. After geometry optimization, the complex system does not have dummy atoms, which makes a barrier between these two molecules at the gas phase studied. These similar concepts have been used earlier by Meng et al. [17] and Turner et al. [18] for ab initio calculations. Quantum chemical calculations were performed using Hartree-Fock (HF) Theory with 6-31G* basis set. The geometry optimizations were carried out using HF/6-31G* basis set. For the same basis set, the fundamental vibrational frequency calculations were carried out to ensure the true minimum. The total electronic energies for Triton X-114 surfactant, MB dye, water, and their complex were corrected with the basis set of superposition error using Boys-Bernardi counterpoise techniques [19]. All theoretical calculations were performed using the Gaussian 03 software package [20].

3. Experimental Details

Triton X-114, purchased from Sigma Life Sciences, India, was used as a nonionic surfactant. It is a high purity (>95%) and water soluble liquid. Triton X-114 (octyl phenol poly (ethylene glycol ether)) contains approximately 8-9 ethoxy units per molecule (density at 298.15 K is 1.058 g·mL^{-1}, Mol. Wt.: 537, λ_{max}: 223 nm) and is abbreviated as Triton X-114. The critical micellar concentration (CMC) of Triton X-114 is 2.1×10^{-4} M at 298.15 K and the cloud point temperature is 297.15 K. MB dye (Mol. Wt.: 319.85, density: 1.757 g·mL^{-1}, λ_{max}: 665 nm) purchased from Nuchem chemicals, Ahmedabad, India, was used as a solute. The electrolytes used were sodium sulphate and calcium chloride (purchased from Paxmy). JASCO UV spectrophotometer was used for measuring dye concentration and surfactant concentration in dilute phase after

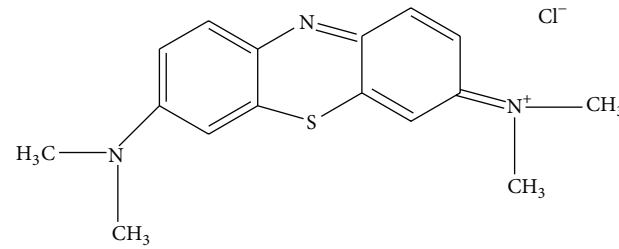

Figure 2: Chemical structure of methylene blue (MB) dye.

phase separation. The density was measured using a 5 mL pycnometer. BROOKFIELD DV-II + PRO viscometer was used to measure the viscosity of the solutions. Refractive index was measured using Abbe Refractometer purchased from Guru Nanak instruments, New Delhi. The chemical structure of Triton X-114 and MB is given in Figures 1 and 2.

50 mL of aqueous micellar solutions was prepared with different concentrations of solute and surfactant. The concentrations of solute (MB) used were 15 ppm, 25 ppm, and 50 ppm. Surfactant concentration was varied from 0.01 M to 0.1 M. 1,000 ppm of dye stock solution was prepared by taking 0.1 g of MB and making it up to 100 mL. Various concentrations of dye solutions were prepared by taking known volumes from stock solution and then diluted appropriately. The calibration of UV spectrophotometer was done using the prepared dye solutions. 50 mL batch solutions of MB and Triton X-114 surfactant were prepared by varying dye concentration and surfactant concentration. The solutions were heated above CPT until phase separation was obtained.

The cloud point of aqueous surfactant solution was determined by heating 50 mL of such molecular solutions in glass tubes. A thermostatic bath made by Technico Laboratory Products Ltd using a Honeywell controller was used to heat the solution. The rate of temperature increase in the water bath was set at 1 K per minute. The cloud point was determined by visual observation of the temperature at which the solution became obvious turbid. While heating, the temperature at which turbidity first appeared was noted down. Heating was continued until the solution became fully turbid. Then, it was cooled down until the turbidity completely disappeared and the solution became transparent.

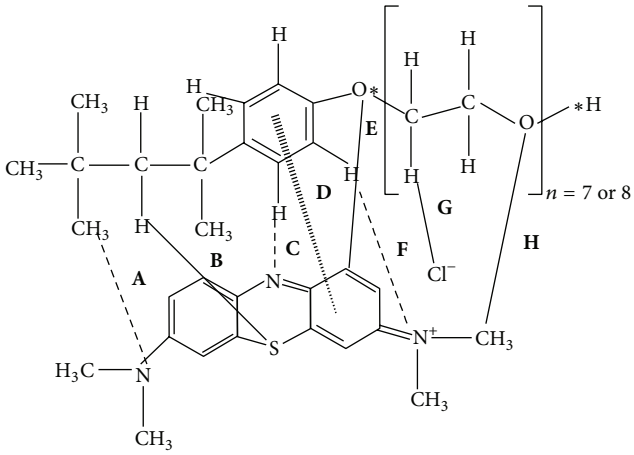

The possible molecular interaction at molecular level:

(**A**) H (surfactant)-N (methylene blue) interaction
(**B**) H (surfactant)-S (methylene blue) interaction
(**C**) H (surfactant)-N (methylene blue) interaction
(**D**) π (surfactant)- π (methylene blue) interaction
(**E**) O (surfactant)-H (methylene blue) interaction
(**F**) H (surfactant)-N (methylene blue) interaction
(**G**) H (surfactant)-Cl (methylene blue) interaction
(**H**) O (surfactant)-H (methylene blue) interaction

(a)

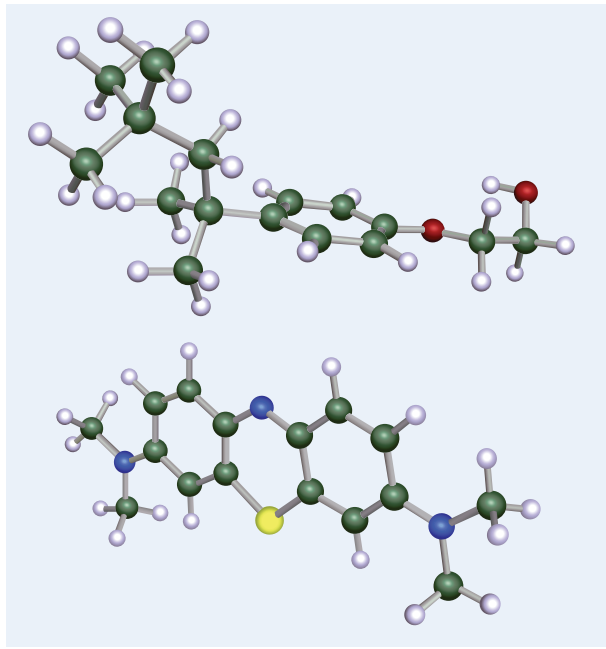

(b)

Figure 3: (a) The possible molecular interaction between Triton X-114 surfactant and methylene blue at molecular level. (b) Optimized complex structure of Triton X-114 with methylene blue dye using HF/6-31G* basis set.

The temperature was also noted down. The average of both readings was taken as the CPT of the solution. The experiments were repeated for different combinations of surfactant and solute concentrations.

50 mL of micellar solution containing MB and Triton X-114 was taken. The different concentrations of MB such as 15, 25, and 50 ppm, the concentration of surfactant, were varied from 0.01 M to 0.1 M. Each set of samples was kept in the thermostatic bath and maintained at the operating temperature for 30 min. Since the surfactant density is 1.058 g·cm^{-3}, therefore, the surfactant rich phase can settle through the aqueous phase. The heated solution was allowed to settle for 1 hr. The volumes of surfactant rich phase and dilute phase were noted down. Then, the concentration of MB in the dilute phase was determined by using UV spectrophotometer. The concentration of surfactant rich phase concentration was obtained from the calculation of material balance. The phase volume ratio, preconcentration factor, distribution coefficient, and extraction efficiency were then determined. The above said parameters were found at different operating temperatures.

4. Results and Discussion

4.1. Binding Energy. The total electronic energy was predicted using HF/6-31G* basis set for Triton X-114 surfactant, Methylene Blue dye, water, Triton X-114 surfactant + Methylene Blue dye (Figures 3(a) and 3(b)), Triton X-114 surfactant + water, Methylene Blue dye + water. This calculation step was performed using Gaussian 03 packages. From this total energy value, the binding energy between Triton X-114 surfactant + MB (Figures 3(a) and 3(b)) and Triton X-114 surfactant + water system was calculated. The binding energy can be defined as the difference between the total electronic energy of the binary system and individual molecules ((a) in Table 1). The binding energy between Triton X-114 surfactant + MB and MB + water is −1222.9620 and −3573.2800 kJ·mole^{-1}, respectively. This value describes that the Triton X-114 surfactant + MB and MB + water system has reliable chemical and physical interaction. However, the binding energy of Triton X-114 surfactant + MB system is low (−1222.9620 kJ·mole^{-1}) when compared to MB + water system (−3573.2800 kJ·mole^{-1}) due to the strength of hydrogen bonds. On the other hand, the presence of MB in water is in ppm level. The binding energy in Triton X-114 surfactant + water is 4303.4720 kJ·mole^{-1}, which indicates that the distance between Triton X-114 surfactant and water molecules is large due to the absence of chemical and physical interaction. In addition, Triton X-114 surfactant is immiscible with water molecules, which is more favorable for effective separation of MB from water. There are also several chemical and physical interactions occurring between Triton X-114 surfactant and MB such as orbital interaction, charge-charge interaction, and hydrogen bond interaction with neutral molecules, van der Waals interaction between

Table 2: Physical properties of coacervate phase at 313.15 and 323.15 K.

Triton X-114 (M)	Density (ρ) ($g \cdot cm^{-3}$)	Refractive index (nD)	Viscosity (μ) (m·Pas)	Excess molar volume (V_E) ($cm^3 \cdot mole^{-1}$)
		313.15 K		
0.01	NA	1.355	NA	NA
0.02	NA	1.358	NA	NA
0.03	1.0110	1.357	NA	−0.10675
0.04	1.0134	1.362	NA	−0.13257
0.05	1.0214	1.363	NA	−0.26556
0.06	1.0258	1.363	NA	−0.35633
0.07	1.0219	1.364	162.2	−0.26946
0.08	1.0233	1.366	164.4	−0.28251
0.09	1.0270	1.377	186.2	−0.35201
0.10	1.0340	1.387	190.0	−0.49725
		323.15 K		
0.01	NA	1.358	NA	NA
0.02	NA	1.360	NA	NA
0.03	NA	1.361	NA	NA
0.04	1.0218	1.364	NA	−0.26332
0.05	1.0240	1.365	NA	−0.29124
0.06	1.0268	1.367	NA	−0.33472
0.07	1.0244	1.370	190.2	−0.27629
0.08	1.0291	1.371	194.4	−0.37310
0.09	1.0322	1.376	193.8	−0.00564
0.10	1.0355	1.379	202.2	−0.49792

alkyl chain, CH-π interaction, π-π interaction, and n-π interaction (Figure 3(a)) [21–24].

4.2. Properties of Dilute Phase and Coacervate Phase. As listed in Table 2, the dilute phase properties were found to be similar to that of water. The dye present in the solution is solubilized in the surfactant micelle present in the coacervate phase. Therefore, the dilute phase only contains small concentration of dye and surfactant, and the major component is water.

Density. The variation of density with surfactant concentration and temperature are given in Table 2. The coacervate phase consists of dye, surfactant, and water molecules. With the increase in surfactant concentration, the surfactant molecules form higher number of micelles, and the size of the micelle also increases [25]. Due to the density difference, the surfactant will settle in the coacervate phase and the surfactant content in the coacervate phase increased. As there are a larger number of micelles, more dye solute will be solubilized in the surfactant micelles. Hence, the density increases with surfactant concentration. With the increase in temperature, the solubility of the dye increased. The maximum amount of solute will be solubilized. The main reason is water molecules escape from the external layers of the micelle. As the water content decreases, the solution becomes very dense.

Viscosity. The variation of viscosity with surfactant concentration and temperature are given in Table 2. The viscosity of Triton X-114 surfactant is 260 cp, which is very high compared to that of water (1 cp). Therefore, as the surfactant concentration increases, the surfactant rich phase becomes more viscous due to molecular attraction between similar structures of the molecules. An increase in the content of water molecules can decrease the viscosity due to the weak hydrogen bond interaction. Thus, at higher temperatures, the viscosity of the solution increases due to the removal of water molecules from the external layers of micelle. It is noted that the viscosity of the mixture strongly depends on the presence of water or moisture.

Refractive Index. It is defined as the ratio of the speed of light in vacuum to the speed of light in the medium. The refractive index increases with surfactant concentration and temperature, as given in Table 2. It can be explained that more dye solubilized at higher temperature and surfactant concentration and there is no mobility of ions in the surfactant rich phase. As the density increases, there is a compact arrangement of the molecules in the phase, and consequently the speed of light through that medium decreases. As

a result, the refractive index increases. Thus, the refractive index strongly depends on the amount of dye present in the coacervate phase. A linear regression was sufficient for a reliable extrapolation for all measured quantities.

4.3. Excess Molar Volume of Dilute Phase and Coacervate Phase. The excess molar volumes for both phases were calculated with the help of measured pure component density by using (b) in Table 1. The value of excess molar volume, V_E, was found to be positive in the dilute phase. In Table 2, it is shown that V_E values are positive, which means that there is an expansion after mixing. That is, the actual volume of the mixture is greater than the volume occupied by the individual components. The physical effects of the dye, surfactant, and water molecules present in the dilute phase contribute to the positive value of V_E due to the presence of physical interactions. Hence, the possible physical interactions are (1) hydrophobic interactions between surfactant hydrocarbon chains dye and water curvature-dependent interfacial effects at the micellar core-water interface, (2) steric and electrostatic interactions between surfactant hydrophilic moieties, and (3) disruption of bonds between the molecules, which also makes positive contributions. As the temperature increases, there will be disruption of H-bond between the surfactant molecule and water molecules, which results in volume expansion and hence positive V_E. Excess molar volume in coacervate phase is illustrated in Figure 8. It is seen that V_E values are negative, which means there is contraction after mixing. The actual volume of the mixture is less than the volume occupied by the individual components. Hence, there is a strong intermolecular force of attraction between the molecules in the surfactant rich phase. The chemical and structural effects of the dye, surfactant, and water molecules make a negative contribution. The packing effects or conformational changes of the molecules in the mixtures are more difficult to categorize. The interstitial accommodation gives negative contributions. The calculated excess molar volume values are shown linearly fit which indicated a high degree of experimental data.

4.4. Effect of Surfactant and Solute Concentrations on CPT. Table 3 shows the effect of solute and surfactant concentrations on cloud point temperature. The experiments were carried out by varying the surfactant concentration from 0.01 M to 0.1 M for 15 ppm, 25 ppm, and 50 ppm solute concentrations. The CPT first decreases and then increases with the increase in surfactant concentration. The decrease in CPT with an increase in surfactant concentration is due to the increase in molecular concentration and the phase separation results from the increased molecular interaction. After 0.06 M surfactant concentrations, the CPT starts to increase. This is because of the formation of structured surfactant Triton X-114-MB system present in the micelles at high surfactant concentrations. More energy is required to remove these "free floating" water molecules, and hence CPT increases with surfactant concentration at higher surfactant concentrations. From Table 3, it can be observed that CPT is increased with increase in solute concentration. Because,

Table 3: CPT at different solute and surfactant concentration.

Triton X-114 (M)	15 ppm	25 ppm	50 ppm
0.01	296.7	297.2	298.2
0.02	296.45	297.05	297.8
0.03	296.3	297.05	297.55
0.04	296.2	296.7	297.55
0.05	296.2	296.2	296.45
0.06	295.4	296.4	296.6
0.07	295.6	296.45	296.8
0.08	296.65	296.85	297.4
0.09	297.25	296.95	297.6
0.10	297.35	297.25	297.7

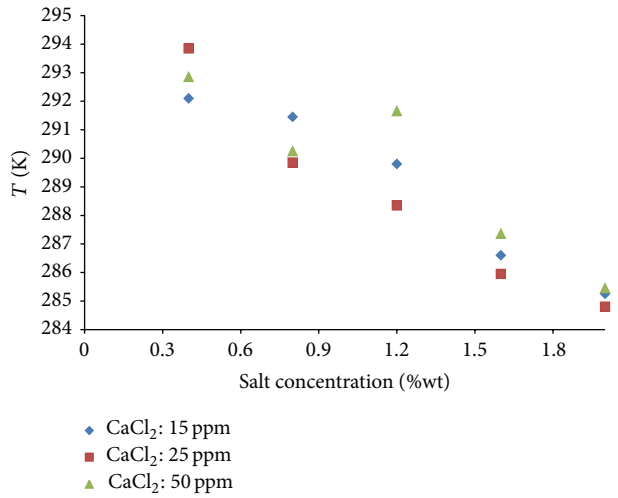

Figure 4: Effect of $CaCl_2$ on CPT at 0.1 M Triton X-114 (R^2 values by linear regression: 0.9613 for 15 ppm, 0.9796 for 25 ppm, and 0.8799 for 50 ppm).

polyoxyethlenated alkyl phenol molecules present in Triton X-114. This hydrophobic part depends on a hydrocarbon chain with different number of carbon atoms and may be linear or branched. It may also contain aromatic rings. Therefore, the surfactant concentration increased and the hydrophobicity of the ligand and of the complex formed on the apparent equilibrium constants in the micellar medium [25, 26].

4.5. Effect of Electrolytes on Cloud Point Temperature. Salts can promote or inhibit the dehydration process and therefore either decrease or increase the cloud point. This behavior is said to be the salting-in and salting-out phenomena. In order to study the salting-out effects, $CaCl_2$ and Na_2SO_4 were used. In Figure 4, the salting out effect of $CaCl_2$ is shown at 0.1 M surfactant concentration. The concentration of salt was varied from 2 to 10 wt%. Figure 5 shows the salting out effect of Na_2SO_4 with salt concentration varied from 0.4 to 2 wt% at surfactant concentration 0.1 M and

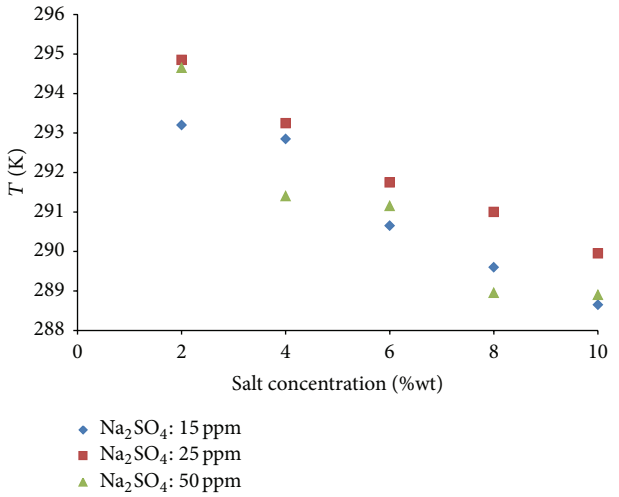

FIGURE 5: Effect of Na_2SO_4 on CPT at 0.1 M Triton X-114 (R^2 values by linear regression: 0.9557 for 15 ppm, 0.9544 for 25 ppm, and 0.837 for 50 ppm).

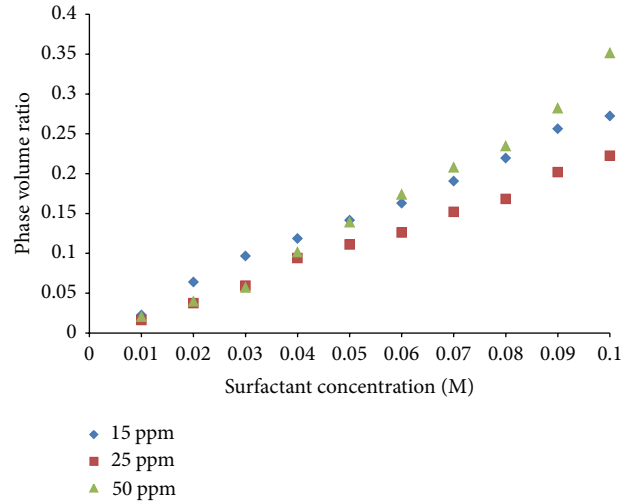

FIGURE 6: Effect of solute and surfactant concentration on phase volume ratio at 323.15 K (R^2 values by linear regression: 0.9956 for 15 ppm, 0.9824 for 25 ppm, and 0.9941 for 50 ppm).

solute concentrations of 15 ppm, 25 ppm, and 50 ppm. In the figure, it is shown that the cloud point decreases with the increase in Na_2SO_4 and $CaCl_2$ concentrations. The addition of certain salts to the nonionic surfactant solution can depress the cloud point temperature by decreasing the availability of nonassociated water molecules to hydrate the ether oxygen's of the polyethylene chains. They convert free water molecules to aggregate water molecules. Along with EO groups, these salts also have a competition for water molecules. From both figures, one can notice that the Na_2SO_4 salt is more effective than $CaCl_2$. The magnitude of the effects of the anions and cations appears to depend on the radius of the hydrated ions; the smaller the radius, the greater the effects. Here, the anion of the added electrolyte appears to have a much greater effect than the cation in decreasing the solubilizing power of water. Since SO_4^{2-} is a polyvalent ion, it will dehydrate water more quickly from the EO chain. Hence, the effect of Na_2SO_4 is greater than $CaCl_2$ [27]. As can be seen from Figures 4 and 5, a linear regression was sufficient for a reliable extrapolation and gave R^2 range: 0.8799–0.9796 for $CaCl_2$ and 0.8370–0.9557 for Na_2SO_4 at 0.1 M of Triton X-114.

4.6. Effect of Operating Variables on CPE Techniques. Experiments were done by changing the operating variables such as solute and surfactant concentration, as well as operating temperature. The effects of these variations on different design parameters such as phase volume ratio (R_v), preconcentration factor (f_c), efficiency (η%), and distribution coefficient (K_d) were investigated. Based on the CPT, the operating temperatures chosen were 303.15, 313.15, 323.15, and 333.15 K for solute concentrations 15 ppm, 25 ppm, and 50 ppm with surfactant varying from 0.01 M to 0.1 M.

4.6.1. Phase Volume Ratio (R_v). The phase volume ratio, R_v, is defined as the ratio of the volume of the surfactant rich phase to that of the aqueous phase ((c) in Table 1). The volumes of the two phases were measured using graduated cylinders. Experiments were conducted for different solute concentrations (15 ppm, 25 ppm, and 50 ppm) with a surfactant varying from 0.01 M to 0.1 M. Figure 12 shows the effect of surfactant and solute concentration in phase volume ratio. From Figure 6, R_v increases with the increase in surfactant concentration and solute concentration. At constant feed dye concentration and operating temperature (323.15 K), R_v increases with surfactant concentration. At higher surfactant concentrations, all the added surfactant will simply go into the surfactant rich phase and the concentration of surfactant in dilute phase being constant at CMC [26, 28–31]. This increases the coacervate phase volume, thereby increasing the phase volume ratio. Solute concentration only has a negligible effect on R_v. The phase volume ratio shows a slight increase in dye concentration at constant temperature. The plotted data shows a reliable linear regression with R^2 values such as 0.9956 (15 ppm), 0.9824 (25 ppm), and 0.9941 (50 ppm).

Figure 7 shows the effect of temperature on phase volume ratio. R_v decreases with temperature. At elevated temperatures, two opposing phenomena occur. The interaction among the Triton X-114 micelles increases due to dehydration from the external layers of micelles, resulting in a decrease in the volume of surfactant rich phase. Also, the increase of micellar aggregation number and micelle sizes results in increased solubilization of MB in the micelles [25, 26]. Depending on the solute (MB) surfactant (Triton X-114) system and the operating conditions, either of these phenomena will be predominant. At lower surfactant concentrations and high operating temperature (333.15 K), the dehydration of water molecules from external micellar layers may be predominant, thereby increasing the dilute phase volume and consequently decreasing the phase volume ratio. The surfactant concentration increases by keeping the operating temperature fixed at 333.15 K (Table 4). The latter phenomena, that is, the increase in micellar number and size, suppresses

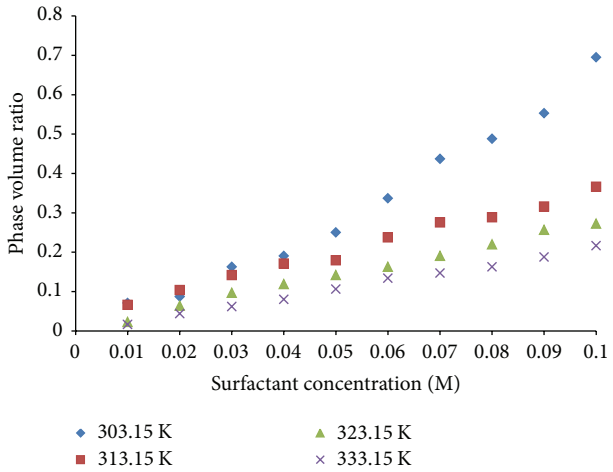

Figure 7: Effect of temperature on the phase volume ratio of solute concentration of 15 ppm (R^2 values by linear regression: 0.9744 for 303.15 K, 0.9896 for 313.15 K, 0.9941 for 323.15 K, and 0.9958 for 333.15 K).

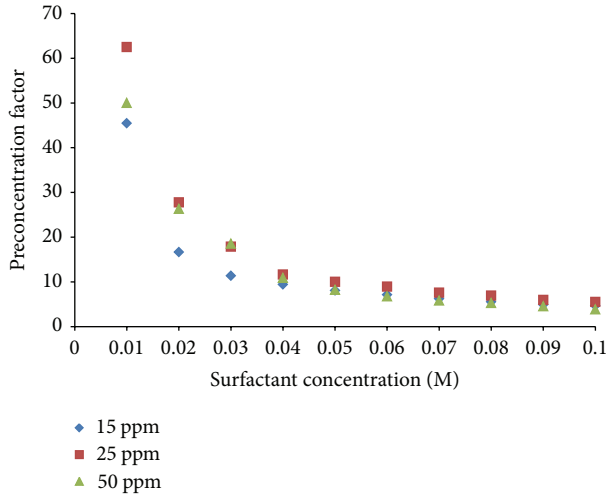

Figure 8: Effect of solute and surfactant concentration on preconcentration factor at 323.15 K (R^2 values by exponential regression: 0.8157 for 15 ppm, 0.8571 for 25 ppm, and 0.9141 for 50 ppm).

the former, thereby increasing R_v. The linear rgression extraplotion was given R^2 value as 0.9744 (303.15 K), 0.9896 (313.15 K), 0.9941 (323.15 K), and 0.9958 (33.15 K).

4.6.2. Preconcentration Factor (f_c). The preconcentration factor, f_c, is defined as the ratio of the volume of bulk solution before phase separation (V_t) to that of surfactant rich phase after phase separation (V_s) ((d) in Table 1). Preconcentration factor is an indication of the ratio of solute concentration in feed to that in the surfactant rich phase. The higher the value of preconcentration factor is, the lesser will be the separation of solute and vice versa. Figure 8 shows the effect of surfactant and solute concentration in preconcentration factor. It is observed that the preconcentration factor decreases with

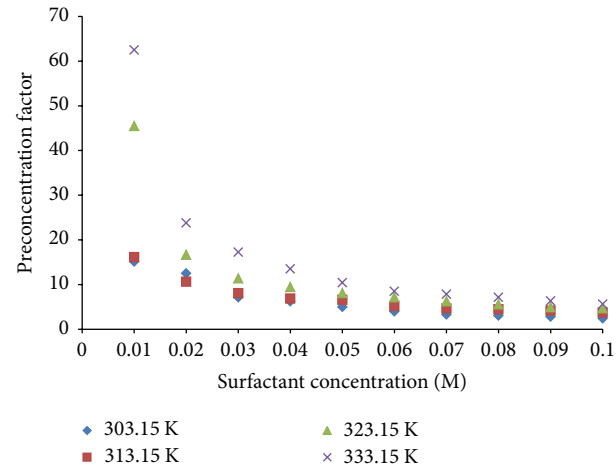

Figure 9: Effect of operating temperature on preconcentration factor at solute concentration of 15 ppm (R^2 values by exponential regression: 0.9155 for 303.15 K, 0.9155 for 313.15 K, 0.8157 for 323.15 K, and 0.8533 for 333.15 K).

the increase in surfactant concentration. As discussed earlier, surfactant rich phase volume increases with increasing surfactant concentration, thereby decreasing f_c [32, 33] and the similar trend is also observed. As shown in Figure 8, f_c increases only marginally with solute concentration. At 50 ppm MB concentration, the surfactant concentration is not enough to solubilized MB in micelles and therefore the trend is below the 25 ppm of MB line. But, the above 0.9% wt of surfactant concentration increased, concentration of micelles increases, and more MB will be solubilized in micelle. On the other hand, further increase in MB concentration only results in an increase of unsolubilized in micelles as a function of surfactant concentration. Therefore, it can be concluded that the ratios of surfactant and MB play an important role in the removal of the dye.

Preconcentration factor is only slightly affected by operating temperature as evident from Figure 9. At higher temperature, micellar aggregation number and size increase, thereby increasing surfactant rich phase volume [25, 26]. On the other hand, dehydration from the external layers of micelles at elevated temperatures reduces the surfactant rich phase volume. These two opposing phenomena act against each other so as to keep the volume of surfactant rich phase almost constant. The linear regression R^2 values were obtained greater than 0.9824 for all ppm and greater than 0.8533 for all temperatures.

4.6.3. Distribution Coefficient (K_d). The distribution coefficient or equilibrium partition coefficient, K_d or K_p, is defined as the ratio of the concentration of solute in surfactant rich phase to that of the concentration of solute in dilute phase ((e) in Table 1). The distribution coefficient increases with the increase in the surfactant concentration and the decrease in solute concentration. The distribution of solute depends on the specific solute (MB) surfactant (Triton X-114) interaction. If there is more interaction, then the distribution

Table 4: Phase volume ratio, preconcentration factor, distribution coefficient, and efficiency at different temperature.

Triton X-114 (M)	Phase volume ratio (R_v)	Preconcentration factor (f_c)	Distribution coefficient (K_d)	Efficiency (η)
		15 ppm at 303.15 K		
0.01	0.0707	15.1515	0.0747	6.9506
0.02	0.0870	12.5000	0.1170	10.4732
0.03	0.1628	7.1429	0.3227	24.3942
0.04	0.1905	6.2500	0.4399	30.5528
0.05	0.2500	5.0000	0.7335	42.3137
0.06	0.3369	3.9683	0.9449	48.5841
0.07	0.4368	3.2895	1.2283	55.1226
0.08	0.4881	3.0488	1.4877	59.8018
0.09	0.5528	2.8090	1.8535	64.9558
0.1	0.6949	2.4390	2.1537	68.2915
		15 ppm at 313.15 K		
0.01	0.0661	16.1290	0.3026	23.2298
0.02	0.1038	10.6383	0.4615	31.5766
0.03	0.1416	8.0645	0.6656	39.9617
0.04	0.1710	6.8493	0.8322	45.4217
0.05	0.1792	6.5789	1.0131	50.3265
0.06	0.2376	5.2083	1.2835	56.2074
0.07	0.2755	4.6296	1.5056	60.0899
0.08	0.2887	4.4643	1.6316	61.9996
0.09	0.3158	4.1667	1.7639	63.8199
0.1	0.3661	3.7313	2.2204	68.9484
		15 ppm at 323.15 K		
0.01	0.0225	45.4545	0.5087	33.7170
0.02	0.0638	16.6667	0.6784	40.4204
0.03	0.0965	11.3636	0.9359	48.3446
0.04	0.1186	9.4340	1.1001	52.3824
0.05	0.1416	8.0645	1.2567	55.6872
0.06	0.1628	7.1429	1.5427	60.6717
0.07	0.1905	6.2500	1.7026	62.9990
0.08	0.2195	5.5556	1.7842	64.0829
0.09	0.2563	4.9020	2.1293	68.0438
0.1	0.2723	4.6729	2.8259	73.8624
		15 ppm at 333.15 K		
0.01	0.0163	62.5000	0.1154	10.3467
0.02	0.0438	23.8095	0.2317	18.8106
0.03	0.0616	17.2414	0.3434	25.5623
0.04	0.0799	13.5135	0.4562	31.3293
0.05	0.1062	10.4167	0.6249	38.4571
0.06	0.1338	8.4746	0.8351	45.5081
0.07	0.1468	7.8125	0.9366	48.3643
0.08	0.1628	7.1429	1.0632	51.5316
0.09	0.1876	6.3291	1.1840	54.2134
0.1	0.2165	5.6180	1.6252	61.9083
		25 ppm at 303.15 K		
0.01	0.0183	55.5556	0.2773	21.7079
0.02	0.0417	25.0000	0.3484	25.8403
0.03	0.0593	17.8571	0.4019	28.6672
0.04	0.1211	9.2593	0.5676	36.2097
0.05	0.1364	8.3333	0.6415	39.0796
0.06	0.1601	7.2464	0.7831	43.9178
0.07	0.1848	6.4103	0.8082	44.6953
0.08	0.2165	5.6180	1.1515	53.5213
0.09	0.2821	4.5455	1.4388	58.9955
0.1	0.3021	4.3103	1.6148	61.7555

Table 4: Continued.

Triton X-114 (M)	Phase volume ratio (R_v)	Preconcentration factor (f_c)	Distribution coefficient (K_d)	Efficiency (η)
		25 ppm at 313.15 K		
0.01	0.0163	62.5000	0.6042	37.6622
0.02	0.0373	27.7778	0.7016	41.2326
0.03	0.0593	17.8571	0.7983	44.3929
0.04	0.0941	11.6279	0.9376	48.3908
0.05	0.1111	10.0000	1.1158	52.7369
0.06	0.1261	8.9286	1.3285	57.0539
0.07	0.1521	7.5758	1.4299	58.8459
0.08	0.1682	6.9444	1.4366	58.9593
0.09	0.2019	5.9524	1.7389	63.4888
0.1	0.2225	5.4945	1.9361	65.9415
		25 ppm at 323.15 K		
0.01	0.0121	83.3333	0.2784	21.7752
0.02	0.0309	33.3333	0.3371	25.2086
0.03	0.0460	22.7273	0.4013	28.6355
0.04	0.0823	13.1579	0.5039	33.5066
0.05	0.1038	10.6383	0.6162	38.1269
0.06	0.1111	10.0000	0.7357	42.3861
0.07	0.1468	7.8125	0.9102	47.6493
0.08	0.1682	6.9444	1.0515	51.2560
0.09	0.1933	6.1728	1.2762	56.0663
0.1	0.2136	5.6818	1.2591	55.7342
		25 ppm at 333.15 K		
0.01	0.0246	41.6667	0.3059	23.4232
0.02	0.0593	17.8571	0.4026	28.7046
0.03	0.0776	13.8889	0.5038	33.5025
0.04	0.1338	8.4746	0.6658	39.9677
0.05	0.1574	7.3529	0.8487	45.9073
0.06	0.1792	6.5789	1.0177	50.4391
0.07	0.2107	5.7471	1.1811	54.1511
0.08	0.2315	5.3191	1.3880	58.1244
0.09	0.2887	4.4643	1.3475	57.4011
0.1	0.3158	4.1667	1.5486	60.7626
		50 ppm at 303.15 K		
0.01	0.0395	26.3158	0.0370	3.5638
0.02	0.0753	14.2857	0.0584	5.5157
0.03	0.1468	7.8125	0.1044	9.4490
0.04	0.2107	5.7471	0.2132	17.5724
0.05	0.2594	4.8544	0.3665	26.8194
0.06	0.3298	4.0323	0.7557	43.0437
0.07	0.4006	3.4965	0.8972	47.2894
0.08	0.4493	3.2258	1.0437	51.0689
0.09	0.6234	2.6042	1.3295	57.0729
0.1	0.7241	2.3810	1.5805	61.2479
		50 ppm at 313.15 K		
0.01	0.0331	31.2500	0.0975	8.8866
0.02	0.0571	18.5185	0.1475	12.8514
0.03	0.0684	15.6250	0.2105	17.3869
0.04	0.1236	9.0909	0.2933	22.6806
0.05	0.1933	6.1728	0.4603	31.5218
0.06	0.2315	5.3191	0.6017	37.5680
0.07	0.2953	4.3860	0.7990	44.4143
0.08	0.3369	3.9683	1.0073	50.1827
0.09	0.3699	3.7037	1.3389	57.2440
0.1	0.4706	3.1250	1.6083	61.6612

Table 4: Continued.

Triton X-114 (M)	Phase volume ratio (R_v)	Preconcentration factor (f_c)	Distribution coefficient (K_d)	Efficiency (η)
		50 ppm at 323.15 K		
0.01	0.0204	50.0000	0.1507	13.0993
0.02	0.0395	26.3158	0.2359	19.0858
0.03	0.0571	18.5185	0.3483	25.8306
0.04	0.1013	10.8696	0.5550	35.6927
0.05	0.1390	8.1967	0.6922	40.9070
0.06	0.1737	6.7568	0.9491	48.6952
0.07	0.2077	5.8140	1.0966	52.3033
0.08	0.2346	5.2632	1.1722	53.9629
0.09	0.2821	4.5455	1.4955	59.9275
0.1	0.3514	3.8462	1.7496	63.6310
		50 ppm at 333.15 K		
0.01	0.0183	55.5556	0.0756	7.0287
0.02	0.0309	33.3333	0.0982	8.9438
0.03	0.0684	15.6250	0.1437	12.5679
0.04	0.0917	11.9048	0.2241	18.3057
0.05	0.1211	9.2593	0.3609	26.5204
0.06	0.1416	8.0645	0.4648	31.7317
0.07	0.1574	7.3529	0.6028	37.6095
0.08	0.1962	6.0976	0.7631	43.2826
0.09	0.2077	5.8140	0.8053	44.6087
0.1	0.2255	5.4348	1.0177	50.4385

coefficient will be high. Figure 10 shows the effect of surfactant and solute concentration on distribution coefficient [32, 33]. The experiments were carried out at 303.15 K, 313.15 K, 323.15 K, and 333.15 K (Table 4). At fixed surfactant and solute concentrations, K_d increases with operating temperature. As the temperature increases, micellar interaction, which is repulsive at lower temperatures, becomes attractive and hence micellar aggregation number increases. This results in increased solubilization of dye into the surfactant rich phase, thus increasing the dye concentration of the phase. Hence, distribution coefficient increases with operating temperature as evident in Figure 11. The experimental data was fitted by linear regression extrapolation and R^2 values are greater than 0.951 for all surfactant concentration and temperatures.

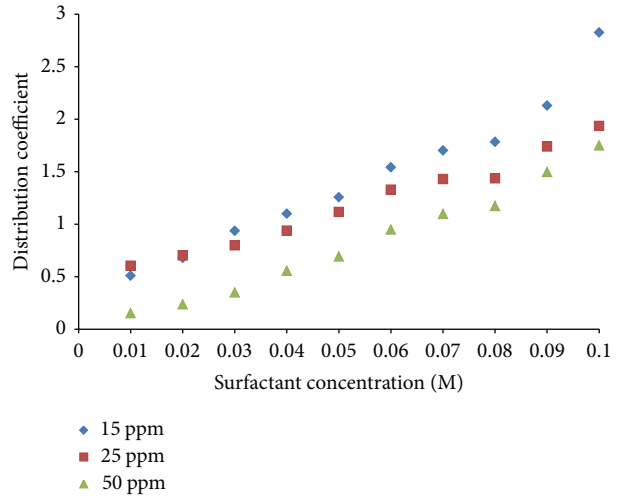

Figure 10: Effect of surfactant and solute concentration on distribution coefficient at 323.15 K (R^2 values by linear regression: 0.951 for 15 ppm, 0.9811 for 25 ppm, and 0.983 for 50 ppm).

4.6.4. Process Efficiency (η). The recovery efficiency of solute, η, can be characterized as the percentage of solute extracted from the bulk solution into the surfactant rich phase ((f) in Table 1). Figures 12 and 13 show the effect of surfactant and solute concentration on extraction efficiency. It increases with the increase in surfactant concentration and decreases with solute concentration. As feed surfactant concentration increases, more dye will be solubilized into the micelles, thereby increasing the efficiency. When solute concentration increases at fixed surfactant concentration and operating temperature, all the added solute will remain in the dilute phase, thereby decreasing the extraction efficiency [26, 28–31].

Experiments were done for various operating temperatures such as 303.15 K, 313.15 K, 323.15 K, and 333.15 K by varying the surfactant concentration and keeping the dye concentration fixed at 15 ppm (Table 4 and Figure 12). As shown in Figure 13, the efficiency of extraction increases with operating temperature. This is due to the increased solubilization of dye resulting from increased micellar size and aggregation number [25, 26]. This similar trend has been observed in the study of Triton X-114-Chrysoidine system [30]. However, after 323.15 K, the effect of temperature is insignificant. It is because dehydration of water occurs from the micelle interface at higher temperatures and micelle interaction increases. As a result, the solubilization of dye cannot occur at the micelle water interface, which decreases

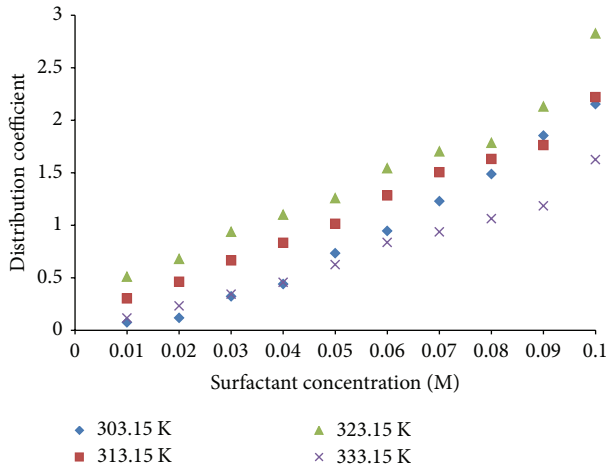

Figure 11: Effect of operating temperature on distribution coefficient at solute concentration of 15 ppm (R^2 values by linear regression: 0.9754 for 303.15 K, 0.951 for 313.15 K, 0.9878 for 323.15 K, and 0.9699 for 333.15 K).

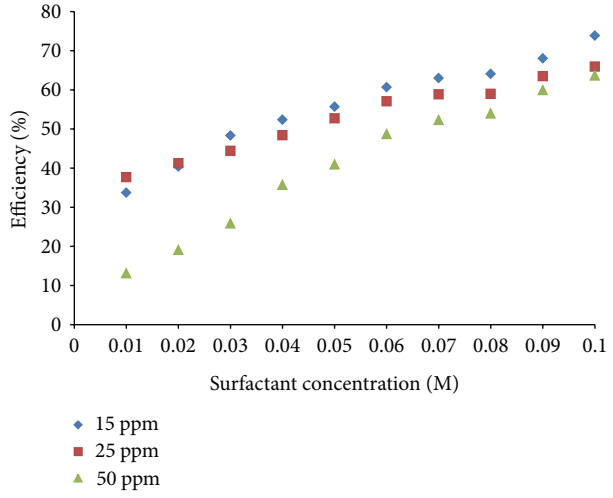

Figure 12: Effect of surfactant and solute concentration on efficiency at 323.15 K (R^2 values by linear regression: 0.9649 for 15 ppm, 0.9797 for 25 ppm, and 0.9746 for 50 ppm).

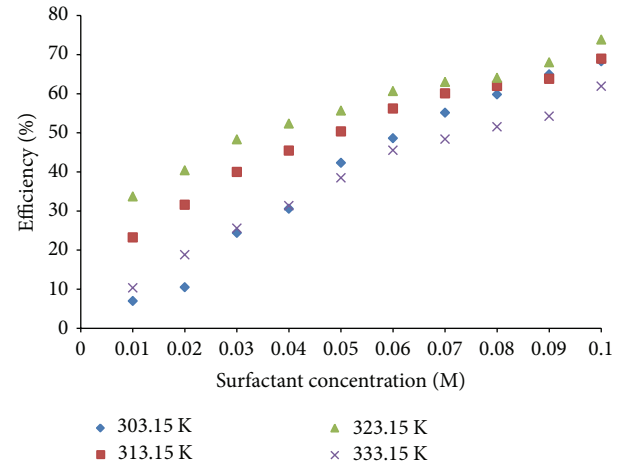

Figure 13: Effect of operating temperature of efficiency at solute concentration of 15 ppm (R^2 values by exponential regression: 0.9745 for 303.15 K, 0.9573 for 313.15 K, 0.9644 K for 323.15 K, and 0.9776 for 333.15 K).

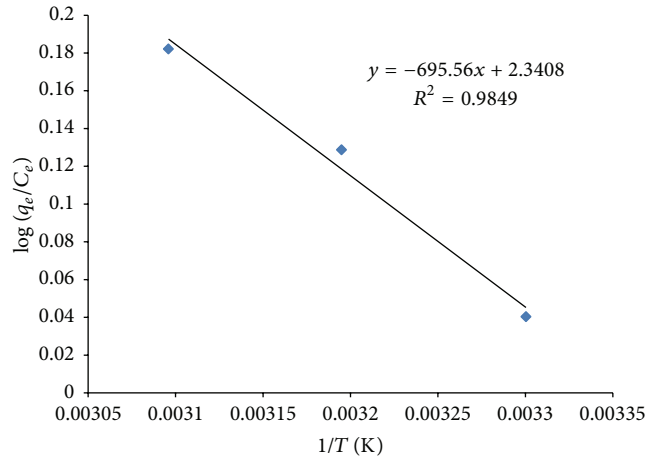

Figure 14: Plot of log (q_e/C_e) versus $1/T$ at surfactant concentration of 0.07 M.

the efficiency. The linear regression extrapolation shows R^2 values such as the following: for solute concentration on efficiency, 0.9649 (15 ppm), 0.9792 (25 ppm), and 0.9746 (50 ppm) and for operating temperature on efficiency, 0.9745 (303.15 K), 0.9573 (313.15 K), 0.9644 (323.15 K), and 0.9776 (333.15 K), respectively.

4.7. Determination of Thermodynamic Parameters. In any process, the study of thermodynamics is important since it is an indication of the feasibility of the process. It serves to identify the extent to which a process can be preceded before attaining equilibrium. Thermodynamic data may also be useful to establish the possible mechanism for CPE of various solutes. The thermodynamic parameters ΔH^0, ΔS^0, and ΔG^0 for the CPE of MB using Triton X-114 were calculated using (g) and (h) in Table 1. ΔS^0 and ΔH^0 were obtained from a plot of $\log(q_e/c_e)$ versus $(1/T)$ from (h) in Table 1. Once these two parameters were obtained, ΔG^0 was determined from (g) in Table 1. $\log(q_e/c_e)$ versus $1/T$ graphs were plotted for various surfactant concentrations as shown in Figure 14, where the slopes and intercepts were obtained to find ΔH^0 and ΔS^0.

The Change in Enthalpy (ΔH^0). The variations of enthalpy change (ΔH^0) during CPE of MB at different concentrations of Triton X-114 are as shown in Figure 15. From the figure, it may be seen that the value of ΔH^0 increases with the Triton X-114 concentration. The positive values of ΔH^0 indicate that the solubilization of dye is endothermic in nature (Table 5). The endothermic nature is also indicated by the increase in the amount of solubilization with temperature. The increase in ΔH^0 value in initial surfactant concentration can be accounted for an increase in solubilization capacity [30]. The

Table 5: Change in entropy, change in enthalpy, and change in Gibbs free energy at different surfactant concentration and different temperature.

Triton X-114 (M)	T (K)	$\log(q_e/C_e)$	ΔS (J/mole K)	ΔH (J/mole)	$-\Delta G$ (J/mole)
0.01	303.15	−0.3306	253.5656	78415.2053	1919.0120
	313.15	0.2769	253.5656	78415.2053	950.8279
	323.15	0.5025	253.5656	78415.2053	3486.4839
	333.15	−0.1417	253.5656	78415.2053	6022.1400
0.02	303.15	−0.4368	230.2635	71928.1536	−2158.3041
	313.15	0.1592	230.2635	71928.1536	144.3312
	323.15	0.3266	230.2635	71928.1536	2446.9665
	333.15	−0.1401	230.2635	71928.1536	4749.6018
0.03	303.15	−0.1723	140.6855	43483.1595	−855.4407
	313.15	0.1422	140.6855	43483.1595	551.4147
	323.15	0.2902	140.6855	43483.1595	1958.2701
	333.15	−0.1452	140.6855	43483.1595	3365.1255
0.04	303.15	−0.1626	120.8778	37434.5773	−808.5972
	313.15	0.1143	120.8778	37434.5773	400.1810
	323.15	0.2354	120.8778	37434.5773	1608.9592
	333.15	−0.1468	120.8778	37434.5773	2817.7375
0.05	303.15	−0.0375	71.8343	21946.4542	−180.6514
	313.15	0.1028	71.8343	21946.4542	537.6920
	323.15	0.1963	71.8343	21946.4542	1256.0353
	333.15	−0.1071	71.8343	21946.4542	1974.3786
0.06	303.15	−0.0067	65.9964	19993.4457	3.4541
	313.15	0.1263	65.9964	19993.4457	663.4178
	323.15	0.2062	65.9964	19993.4457	1323.3815
	333.15	−0.0603	65.9964	19993.4457	1983.3452
0.07	303.15	0.0403	44.8196	13317.9861	262.3618
	313.15	0.1287	44.8196	13317.9861	710.5581
	323.15	0.1821	44.8196	13317.9861	1158.7544
	333.15	−0.0774	44.8196	13317.9861	1606.9507
0.08	303.15	0.0655	25.6553	7394.6262	378.9162
	313.15	0.1056	25.6553	7394.6262	635.4688
	323.15	0.1444	25.6553	7394.6262	892.0213
	333.15	−0.0804	25.6553	7394.6262	1148.5739
0.09	303.15	0.1098	20.0911	5548.8418	538.7604
	313.15	0.0883	20.0911	5548.8418	739.6713
	323.15	0.1702	20.0911	5548.8418	940.5823
	333.15	−0.0848	20.0911	5548.8418	1141.4932
0.1	303.15	0.1293	38.3460	10958.1008	660.7315
	313.15	0.1425	38.3460	10958.1008	1044.1913
	323.15	0.2472	38.3460	10958.1008	1427.6511
	333.15	0.0070	38.3460	10958.1008	1811.1109

experimental data was fit with linear regression and 0.8383 R^2 value.

The Change in Entropy (ΔS^0). The variations of entropy change (ΔS^0) at different concentrations of Triton X-114 are shown in Figure 16. The entropy changes are positive (Table 5), which reflects a good affinity of dye molecules towards surfactant micelles. For all the systems, the change in entropy (ΔS^0) increases with surfactant concentration. Entropy depends on insolubilized dye molecules and free surfactant molecules in the CPE system. The increase in ΔS^0 value in surfactant concentration is due to the increase of free surfactant molecule in the dilute phase. On the other hand, CMC of the surfactant molecule decreases with the increase in dye concentration at a fixed surfactant concentration. This similar trend has been observed by Purkait et al. [31]. The linear regression R^2 value is 0.8036.

The Change in Gibbs Free Energy (ΔG^0). The values of Gibbs free energy (ΔG^0) with temperature have been calculated by knowing the enthalpy of solubilization (ΔH^0) and the entropy of solubilization (ΔS^0) at different surfactant concentrations. From Figure 17, ΔG^0 increases with temperature and decreases with surfactant concentration. In all the cases calculated, the values of free energy changes ΔG^0 were found to be negative as shown in Figure 17 and it is given in Table 5.

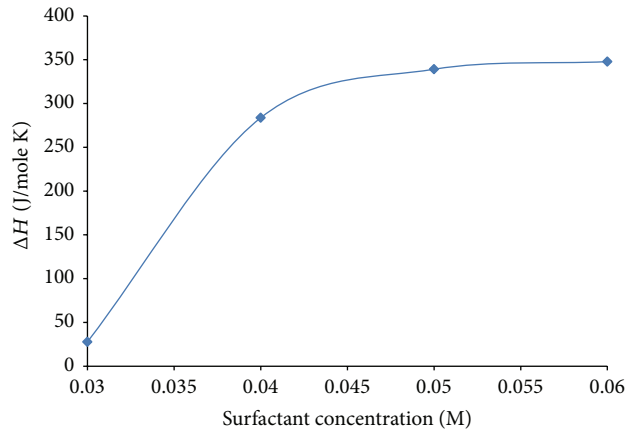

Figure 15: Change in enthalpy versus surfactant concentration in 15 ppm of dye (R^2 value is 0.8383).

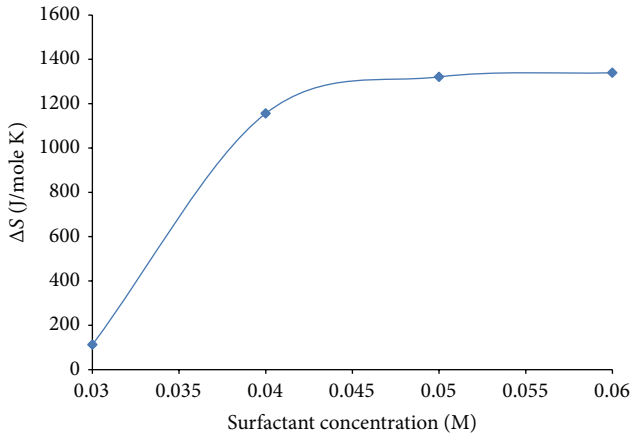

Figure 16: Change in entropy versus surfactant concentration in 15 ppm of MB dye (R^2 value is 0.8036).

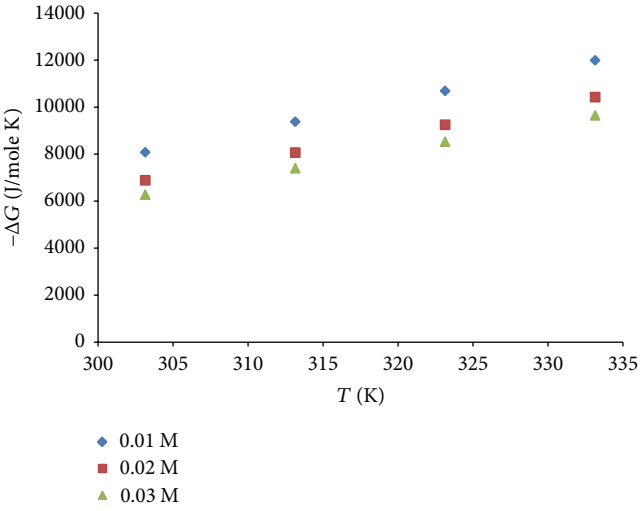

Figure 17: Change in Gibbs free energy versus temperature at 0.01 M, 0.02 M, and 0.03 M of MB dye (R^2 value is 1 for all).

The negative values of ΔG^0 indicate that the dye solubilization process is spontaneous and thermodynamically favorable. The increase in negative values of ΔG^0 with temperature implies the greater driving force of solubilization, which is confirmed by the greater extent of dye extraction with the increase in temperature [31]. The linear relationship between negative ΔG^0 as function of temperature was obtained R^2 value as unity.

5. Conclusions

A quantum chemical calculation in this study of the binding energy between Triton X-114 surfactant and MB/Triton X-114 surfactant + water/MB + water system has been investigated. The results show that the interactions of Triton X-114 surfactant + MB and MB + water depend mainly on hydrogen bond interaction, CH-π interaction, and π-π interaction. The absorption capacity of MB dye in the surfactant depends strongly on the structure, strength of hydrogen bonding, and a hetero atom in the surfactant. However, the calculated binding energy is directly proportional to the distance, which shows that the hydrogen bond interaction is the dominant interaction in the attractions. In addition, the cloud point extraction was carried out at a cloud point temperature, where the mixture of surfactant, water, and MB exhibited two phases. The density, viscosity, and refractive index of pure and two phases of the binary mixture were measured. From this measured density, the excess molar volume has been calculated, which confirmed the type of interaction occurred between similar and dissimilar compounds in two different phases. Furthermore, the design parameters and thermodynamics feasibility factors such as phase volume ratio, preconcentration factor, distribution coefficient, the efficiency of the process, change in enthalpy (ΔH^0), change in entropy (ΔS^0), and change in Gibbs free energy (ΔG^0) have been investigated. It is concluded that the negative value of ΔG^0 indicates that extraction is spontaneous and thermodynamically favorable.

Nomenclature

CPE: Cloud point extraction
CPT: Cloud point temperature
MB: Methylene blue
TX-114: Triton X-114
BE: Binding energy
V_E: Excess molar volume
x_i: Moles of component i
M_i: Molecular weight of component i
ρ_i: Density of component in g·cm^{-3}
ρ_{mix}: Density of mixture in g·cm^{-3}
R_v: Phase volume ratio
V_s: Volume of surfactant rich phase
V_w: Volume of aqueous phase
f_c: Preconcentration factor
V_t: Volume of bulk solution before phase separation

V_s: Surfactant rich phase after phase separation
K_d: Distribution coefficient
C_s: Concentration of solute in surfactant rich phase
C_w: Concentration of solute in dilute phase
η: Efficiency of solute
C_0: Initial concentration of solute in micellar solution
C_W: Concentration of solute in dilute phase
V_t: Total feed volume
V_s: Volume of surfactant rich phase
ΔG^0: Change in Gibbs free energy
ΔS^0: Change in entropy
ΔH^0: Change in enthalpy
T: Temperature in K
q_e: Moles of dye solubilized per mole of non-ionic surfactant
C_e: Equilibrium concentration of dye (moles/L) before the completion of two phases
A: Moles of dye solubilized in the micelles
V_0: Volume of feed solution
V_d: Dilute phase after CPE
C_s: Concentration of surfactant in feed.

Conflict of Interests

The authors declare that there is no conflict of interests regarding the publication of this paper.

Acknowledgments

The work is partially supported by the Tamil Nadu State Council for Science and Technology (TNSCST/S&T project/VR/ES/2009-2010). The authors wish to thank the Tamil Nadu State Council Science and Technology for their financial support.

References

[1] M. I. El-Khaiary, "Kinetics and mechanism of adsorption of methylene blue from aqueous solution by nitric-acid treated water-hyacinth," *Journal of Hazardous Materials*, vol. 147, no. 1-2, pp. 28–36, 2007.

[2] D. Ghosh and K. G. Bhattacharyya, "Adsorption of methylene blue on kaolinite," *Applied Clay Science*, vol. 20, no. 6, pp. 295–300, 2002.

[3] E. Lorenc-Grabowska and G. Gryglewicz, "Adsorption characteristics of Congo Red on coal-based mesoporous activated carbon," *Dyes and Pigments*, vol. 74, no. 1, pp. 34–40, 2007.

[4] M. Doğan, H. Abak, and M. Alkan, "Adsorption of methylene blue onto hazelnut shell: kinetics, mechanism and activation parameters," *Journal of Hazardous Materials*, vol. 164, no. 1, pp. 172–181, 2009.

[5] N. D. Gullickson, J. F. Scamehornand, and J. H. Harwell, *Liquid-Coacervate Extraction-Surfactant Based Separation Processes*, Marcel Dekker, New York, NY, USA, 1989.

[6] W. Kimchuwanit, S. Osuwan, J. F. Scamehorn, J. H. Harwell, and K. J. Haller, "Use of a micellar-rich coacervate phase to extract trichloroethylene from water," *Separation Science and Technology*, vol. 35, no. 13, pp. 1991–2002, 2000.

[7] M. J. Rosen, *Surfactant and Interfacial Phenomena*, John Wiley & Sons, New York, NY, USA, 2nd edition, 2000.

[8] U. S. Vural, V. Muradoglu, and S. Vural, "Excess molar volumes, and refractive index of binary mixtures of glycerol + methanol and glycerol + water at 298.15 k and 303.15 K," *Bulletin of the Chemical Society of Ethiopia*, vol. 25, no. 1, pp. 111–118, 2011.

[9] R. Francesconi, F. Comelli, and C. Castellari, "Excess molar enthalpies and excess molar volumes of binary mixtures containing dialkyl carbonates + anisole or phenetole at (288.15 and 313.15) K," *Journal of Chemical and Engineering Data*, vol. 45, no. 4, pp. 544–548, 2000.

[10] U. S. Vural, H. Yuruk, and V. Muradoglu, "Excess volumetric properties of mixtures epichlorohydrine + acetone or chloroform at 291.15 and 296.15 K," *Russian Journal of Physical Chemistry A*, vol. 77, no. 7, pp. 1091–1094, 2003.

[11] U. S. Vural, V. Muradoglu, and H. Yuruk, "Excess volumetric properties of mixtures (epichlorohydrine + toluene and epichlorohydrine + xylene) at 298.15, 308.15, 323.15, and 338.15 K," *Russian Journal of Physical Chemistry*, vol. 78, p. 33, 2004.

[12] U. S. Vural, "Excess molar volumes and viscosities of binary mixtures of epichlorohydrine and alcohols," *Russian Journal of Physical Chemistry A*, vol. 79, no. 7, pp. 1096–1101, 2005.

[13] R. K. Hind, E. McLaughlin, and A. R. Ubbelohde, "Structure and viscosity of liquids. Viscosity-temperature relationships of pyrrole and pyrrolidine," *Transactions of the Faraday Society*, vol. 56, pp. 331–334, 1960.

[14] M. Domínguez, J. Pardo, M. C. López, F. M. Royo, and J. S. Urieta, "Viscosities of the ternary mixture (1-butanol + n-hexane + 1-butylamine) at the temperatures 298.15 and 313.15 K," *Fluid Phase Equilibria*, vol. 124, no. 1-2, pp. 147–159, 1996.

[15] I. Frenkel, *Kinetic Theory of Liquids*, Oxford University Press, London, UK, 1946.

[16] G. Schaftenaar and J. H. Noordik, "Molden: a pre- and post-processing program for molecular and electronic structures," *Journal of Computer-Aided Molecular Design*, vol. 14, no. 2, pp. 123–134, 2000.

[17] Z. Meng, A. Dölle, and W. R. Carper, "Gas phase model of an ionic liquid: semi-empirical and ab initio bonding and molecular structure," *Journal of Molecular Structure*, vol. 585, pp. 119–128, 2002.

[18] E. A. Turner, C. C. Pye, and R. D. Singer, "Use of ab initio calculations toward the rational design of room temperature ionic liquids," *Journal of Physical Chemistry A*, vol. 107, no. 13, pp. 2277–2288, 2003.

[19] S. Boys and F. Bernardi, "The calculation of smaller molecular intercations by the differences of separate total energies, some procedure with reduced errors," *Molecular Physics*, vol. 19, pp. 553–566, 1970.

[20] M. J. Frisch, G. W. Trucks, H. B. Schlegel et al., *Gaussian 03*, Revision C.02, Gaussian, Pittsburgh, Pa, USA, 2004.

[21] A. M. Fernandes, M. A. A. Rocha, M. G. Freire, I. M. Marrucho, J. A. P. Coutinho, and L. M. N. B. F. Santos, "Evaluation of cation-anion interaction strength in ionic liquids," *The Journal of Physical Chemistry B*, vol. 115, no. 14, pp. 4033–4041, 2011.

[22] R. Lü, J. Lin, and Z. Qu, "Theoretical study on interactions between thiophene/dibenzothiophene/cyclohexane/toluene and 1-methyl-3-octylimidazolium tetrafluoroborate," *Structural Chemistry*, vol. 24, no. 2, pp. 507–515, 2013.

[23] O. Castellano, R. Gimon, and H. Soscun, "Theoretical study of the σ-π and π-π interactions in heteroaromatic monocyclic molecular complexes of benzene, pyridine, and thiophene dimers: implications on the resin-asphaltene stability in crude oil," *Energy and Fuels*, vol. 25, no. 6, pp. 2526–2541, 2011.

[24] R. Anantharaj and T. Banerjee, "Quantum chemical studies on the simultaneous interaction of thiophene and pyridine with ionic liquid," *AIChE Journal*, vol. 57, no. 3, pp. 749–764, 2011.

[25] R. Carabias-Martínez, E. Rodríguez-Gonzalo, B. Moreno-Cordero, J. L. Pérez-Pavón, C. García-Pinto, and E. Fernández Laespada, "Surfactant cloud point extraction and preconcentration of organic compounds prior to chromatography and capillary electrophoresis," *Journal of Chromatography A*, vol. 902, no. 1, pp. 251–265, 2000.

[26] A. Kitahara, K. Watanabe, K. Kon-no, and T. Ishikawa, "Mechanism of solubilization of water by oil-soluble surfactant solutions I. Anionic surfactants. Part II. Cationic Surfactants, appears on pp. 1–5 of this issue," *Journal of Colloid And Interface Science*, vol. 29, no. 1, pp. 48–54, 1969.

[27] M. K. Purkait, S. S. Vijay, S. DasGupta, and S. De, "Separation of congo red by surfactant mediated cloud point extraction," *Dyes and Pigments*, vol. 63, no. 2, pp. 151–159, 2004.

[28] M. K. Purkait, S. Das Gupta, and S. De, "Determination of design parameters for the cloud point extraction of congo red and eosin dyes using TX-100," *Separation and Purification Technology*, vol. 51, no. 2, pp. 137–142, 2006.

[29] M. K. Purkait, S. Das Gupta, and S. De, "Determination of thermodynamic parameters for the cloud point extraction of different dyes using TX-100 and TX-114," *Separation and Purification Technology*, vol. 244, pp. 130–138, 2009.

[30] M. K. Purkait, S. DasGupta, and S. De, "Performance of TX-100 and TX-114 for the separation of chrysoidine dye using cloud point extraction," *Journal of Hazardous Materials*, vol. 137, no. 2, pp. 827–835, 2006.

[31] M. K. Purkait, S. Das Gupta, and S. De, "Cloud point extraction of toxic eosin dye using Triton X-100," *Water Research*, vol. 39, pp. 3885–3890, 2005.

[32] B. Yao and L. Yang, "Equilibrium partition of polycyclic aromatic hydrocarbons in cloud point extraction with a silicone surfactant," *Journal of Colloid and Interface Science*, vol. 319, no. 1, pp. 316–321, 2008.

[33] D. Sicilia, S. Rubio, and D. Pérez-Bendito, "Evaluation of the factors affecting extraction of organic compounds based on the acid-induced phase cloud point approach," *Analytica Chimica Acta*, vol. 460, no. 1, pp. 13–22, 2002.